

## **Aerodynamic Performance Degradation Induced by Ice Accretion. PIV Technique Assessment in Icing Wind Tunnel.**

**Fabrizio De Gregorio<sup>1</sup>**

1: LMSA/IWTU laboratory, Centro Italiano Ricerche Aerospaziali (CIRA), Capua, Italy, f.degregorio@cira.it

---

**Abstract** The aim of the present paper is to consider the use of PIV technique in an industrial icing wind tunnel and the potentiality/advantages of applying PIV technique to this specific field. Scope of icing wind tunnels is to simulate the aircraft flight condition through cloud formations. In this operational condition ice accretions appear on the aircraft exposed surfaces due to the impact of the water droplets present in the clouds and the subsequent solidification. The investigation of aircraft aerodynamic performances and flight safety in icing condition is a fundamental aspect in the phase of design, development and certification of new aircrafts. The description of this peculiar ground testing facility is reported.

The assessment of PIV in CIRA-IWT has been investigated. Several technological problems have been afforded and solved developing the components of the measurement system, as the laser system and the recording apparatus, both fully remotely controlled, equipped with several traversing mechanism and protected by the adverse environment conditions (temperature and pressure). The adopted solutions are described.

Furthermore a complete test campaign on a full scale aircraft wing tip, equipped with moving slat and de-icing system has been carried out by PIV. Two regions have been investigated. The wing leading edge area has been studied with and without ice accretion and for different cloud characteristics. The model was settled in high lift condition with extended slat and medium angle of attack. Scope of this measurement is detecting the droplet trajectories, evaluate the collection efficiency, evaluate the aerodynamic flow field distortion due to the ice formation on the extended slat region.

The second region was aimed to investigate the wing wake behaviour. The measurements were aimed to characterise the wake for the model in cruise condition and null angle of attack without ice formation and during the ice formation in order to evaluate the drag coefficient increasing by the evaluation of the loss of momentum.

---

### **1. Introduction**

Aggregation of ice on the exposed aerodynamic component of the vehicles is a major hazard for flying. The flow field perturbation due to ice accretion, the degradation of the aerodynamic performance or the choking of the engine inlets are critical aspects for the performance and safety of airplanes and helicopters. The investigation of the icing accretion problematic requests big effort in the experimental as well in the numerical simulation. In the past and nowadays extended flight campaign have been performed in order to better understand the composition of the clouds. The clouds are mainly characterised by two parameters, the liquid water contents (LWC), indicating the concentration of water and by the Mean Volume Diameter (MVD), reporting the mean size of the droplets. These two parameters together with the air static temperature, the static pressure and the flight condition and the geometry of the affected surfaces govern the type of ice formation and relative hazard degree that can be encountered.

The effect of the influence of the ice accretion on the aerodynamic behaviour has been investigated by performing several flight test. One of the earliest successful attempts to measure the effect of ice accretion was that of Preston and Backman in 1948. In one flight resulted an increment of 81% of parasite drag and almost the complete lost of controlling. The effect of ice on the performance of high performance piston propeller general aviation aircraft has been presented by Leckman 1971.

Leckman estimated for the Cessna Centurion a drag coefficient rise of  $\Delta C_{D0} = 0.055$  (i.e. 275% increase) with no ice protection and 0.0179 (09% increase) with ice protection system operating due to residual ice on unprotected surfaces. Lift was also affected. Flight test data increased the stall speed from 75 mph clean to 102 mph at zero flap and from 65 to 83 mph at 30 degree flap deflection.

Larger data set has been obtained by NASA Glenn Research centre on the Twin Otter aircraft as summarised by Bragg & all 2000. Tests in natural icing as well as test with simulated icing aimed to investigate the behaviour of the stability derivatives have been performed. As results of NASA research, it is clear that ice accretion affects the longitudinal and lateral static stability and control of the aircraft. This effect occurs even at low angle of attack and high power setting, condition typical of cruise. A typical reduction in stability or control was 10%. There is also evidence that the effects of ice are more significant at large angle of attack near stall where significant early flow separation occurs due to the ice.

Flight test are extremely expensive and potentially dangerous so many investigations are conducted in ground facility. For investigating the effect on the aerodynamic coefficients, on the stability derivatives of the ice formation test are conducted in aerodynamic wind tunnels mounting on the model simulated ice shape. These activities are anticipated by test in icing facilities in order to evaluate the ice formation shape for the selected flying condition.

Bragg & Gregorek 1992 predicted the aerodynamic effects of ice on a typical subsonic airfoil by means of analytical and experimental investigations. The analytic method predicted the size and shape of rime ice accretion, and the simulated ice shape was tested in the wind tunnel with a smooth surface and with a roughness equivalent to the natural rime ice accretion. In this way the effects of ice shape and roughness on the aerodynamic coefficients were isolated. Bragg & Coirier 1986 conducted an experimental program to measure the aerodynamic characteristics of a NACA 0012 airfoil with simulated glaze ice shape. The model was also instrumented with a distribution of surface taps to provide detailed information around the ice shapes, where flow separation occurs. As expected, airfoil lift and drag were severely affected by the ice shape. Cuerno & all 1997 investigated the flow field over a clean NACA 0012 and simulated rime and glaze ice accretions at low Reynolds number ( $Re=140000$ ), using laser Doppler velocimetry: velocity profiles on the upper surface at several angles of attack were provided. The existence of separation bubbles at angles of attack much lower than in the clean airfoil, for both rime and glaze ice shapes, was reported.

De Gregorio & all 2001 studied a NACA 0012 airfoil affected by rime, mixed and glaze ice shapes at 200.000 Reynolds number. Together with load measurements, PIV investigation was applied in order to evaluate by the flow characterisation the lift and drag coefficient. Comparison between 3 component balance and aerodynamic coefficient obtained by PIV results presented remarkable agreement.

Starting by this experience the basic idea was to apply PIV technique directly during icing test in the CIRA IWT facility in order to evaluate directly the aerodynamic behavior skipping subsequent aerodynamic test. By measuring the flow field around and downstream the model it is possible to obtain information on the aerodynamic characteristics, on the effectiveness of the de/anti icing systems, on the cloud droplets trajectories together with the flow streamlines and their perturbation during the ice accretion phase. Starting from the droplet trajectories is possible to evaluate the collection efficiency parameter that governs the amount of ice accretion on the exposed surface. Typically during icing running the ice accretion shape is possible to be evaluate only at the end of the run, information about the evolution of the accretion in time are lost. These information are fundamental for cfd code validation. If performing PIV measurement in a industrial wind tunnel is still a challenge, the utilisation in an icing wind tunnel presents some additional difficulties.

Together with the other classical problems the researchers has to deal with: low air temperature, 100% of air relative humidity (moisture and corrosion problems), static pressure conditions. In icing conditions the PIV measurement are carried out using as seeding particles the droplets of the generated clouds. This comports some limitations on the quality of the seeding and on the applicability for some cloud conditions. A preliminary test campaign has been conducted in order to demonstrate the assessment of PIV in the CIRA IWT testing the extreme operating condition of the tunnel in terms of cloud, temperature, speed and static pressure. The PIV instrumentation has been tested in empty test section and downstream the icing blade probe.

Subsequently an experimental test campaign has been carried out on a full scale aircraft wing tip equipped with moving slat and de-icing system. The region in proximity of the wing leading edge has been investigated. Measurement in cruise condition (retracted slat) and in high lift condition (extended slat) have been performed in order to evaluate the disturb and eventually the flow separation due to the ice formation. In particularly the collection efficiency has been investigated.

The measurement has been devoted to characterise the flow field downstream the wing for wake characterisation. Starting by the initial condition of clean model, the flow field measurement have been conducted, during the icing formation process in order to evaluate the drag increasing due to the ice formation. This paper presents the experimental set up, the technological problems that have been afforded and solved, the performed measurements and the obtained results.

## 2. Experimental apparatus

The experimental apparatus, including the test facility, test models and instrumentation are described in the following.

### 2.1 Icing Wind Tunnel (IWT)

The CIRA IWT has been in operation since 2002. The IWT facility is a closed loop circuit, refrigerated wind tunnel with three interchangeable test sections and one Open Jet. A sketch of the IWT layout is shown in Figure 1. As many conventional wind tunnels, the IWT is fan driven. The fan and the fan drive are located downstream of corner 2, in the back leg. Downstream of the fan diffuser, a twin row heat exchanger is located to provide low temperature operation capability. The facility settling chamber is fitted with a honeycomb for reducing large scale eddies and ensures flow straightening.

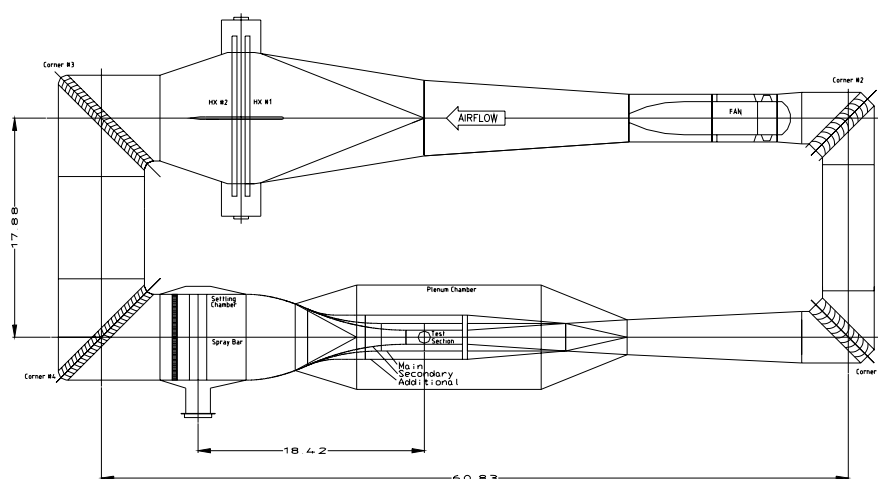


Figure 1: CIRA-IWT layout

Downstream of the honeycomb, an interchangeable section provides the possibility to install either: A) a spray bar module for generating the artificial cloud for icing tests or B) a screen module when

lower turbulence airflow is necessary for high quality aerodynamic testing.

Downstream of the fixed contraction, the test section leg is made up of two interchangeable components (movable contraction + test section) and one adjustable component (collector diffuser). The maximum speed achievable in the IWT depends upon the selected configuration. Mach number up to 0.4 can be achieved using the main test section ( $2.25 \times 2.35 \text{ m}^2$ ), Mach 0.7 in the secondary test section ( $1.15 \times 2.35 \text{ m}^2$ ) and Mach 0.25 in the additional test section ( $3.60 \times 2.35 \text{ m}^2$ ).

Air flow refrigeration is obtained via a twin row heat exchanger (HX) located in the back leg, upstream of the third corner. The minimum temperature achievable is  $-32^\circ\text{C}$  in the main test section and in the additional test section. The secondary test section can get down to  $-40^\circ\text{C}$ . The HX is also capable to control the air relative humidity (RH) in a range from 70% to 100%, through a cooling-heating cycle and steam injection. In addition, an evacuation/pressurisation air system allow the pressure to be regulated from 39000 Pa (abs), corresponding to an altitude of 7000 m, up to 145000 Pa (abs).

## 2.2 Test model

During the first phase, PIV assessment, the measurements have been performed in the empty secondary test section and in the wake of the icing blade probe. This probe is composed by a steel blade of prefixed sizes aimed to measure the LWC value of the cloud measuring the thickness of the ice accreted on the blade. The blade was mounted on the side wall at the centre line high as shown in Figure 2. The blade is shielded by a cover while the requested cloud conditions are obtained.



Figure 2: Icing blade mounted in the secondary TS



Figure 3: Swept wing mounted in the additional TS

The measurement campaign has been carried out on a full scale tip wing. The wing has been mounted in the additional TS due the large dimensions. The model represents the extremity of a swept wing with 3.18 meter span wise and  $32^\circ$  degree of swept angle. The model is equipped of movable slat with hot air de-icing system (piccolo tube). For the present work the de-icing system was not used. The model was mounted on a motorised turn table allowing an incidence angle from  $-15^\circ$  to  $+15^\circ$ .

## 2.3 PIV system

The icing wind tunnel due to its characteristics to be a pressurised circuit is equipped of a large plenum chamber containing the test section. All the PIV recording and illuminating instrumentation was installed inside the plenum. The plenum presents the same characteristics of total temperature, total pressure and Humidity of the test section. For this reason the instrumentation has been mounted inside some devoted casings that maintain the temperature and pressure condition in the range of the operating parameters.

The illuminating system is composed by two Nd-Yag head resonators providing each 200 mJ pulse energy at 532nm wave length with 10 Hz repetition rate. Each laser head has a devoted power supplier. The two power suppliers together with the control unit of the temperature resistance and motor control are located inside a protecting casing. This one is connected with the laser head by means 5 meter long umbilical cable thermal isolated as well. In this way the laser head can be easily located close to the selected optical access while the power supplier casing, much heavier is located on the plenum walking way. The recombined beams by means an alignment mirror are directed inside a mechanical optical arm of 2.5 m length. At the end of the arm the optics generating the light sheet are mounted inside a dedicate housing. The optical head is thermal controlled in order to avoid moisture on the exit windows. The alignment mirror and the spherical lens for adjust the light sheet focusing distance are equipped of servo motors remotely controlled by PC. Figure 4 shows the power supply unit on the wind tunnel passage way, figure 5 shows the laser head with the optical arm mounted on the ceiling of the additional TS and figure 6 illustrates a detail of the optical head mounted outside one of the windows present on the ceiling of the TS.



Figure 4: Laser power supply unit

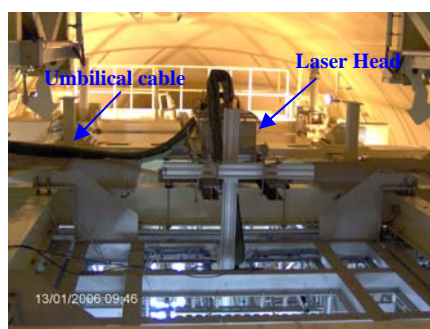


Figure 5: Laser head

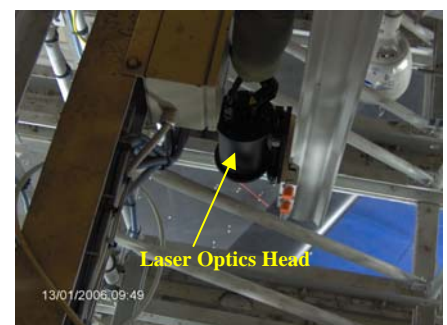


Figure 6: Light sheet optics

The recording system is composed by two 1280x1024 pixel resolution CCD camera. The cameras are located inside special housings that are controlled in temperature. The cameras are equipped with focusing remote systems. Nitrogen is supplied on the windows in order to avoid moisture problem.



Figure 7: Camera housing



Figure 8: PIV Control station

Figure 7 shows the two camera housings mounted outside the side wall of the additional TS. The instrumentation condition, the synchronisation of the camera with laser pulses, the laser energy intensity, the alignment of the laser beam, the camera focusing and the focusing distance of the light sheet are all parameters fully remotely controlled. Figure 8 illustrates the control and recording station of the PIV system, installed in the IWT control room. For PIV measurement the seeding quality is a crucial aspect. Good signal to noise ratio is obtained for right density (10 particles for interrogation windows), uniform concentration and small size particles. For icing test instead of the classical DEHS or olive oil seeding particles, the water

droplets of cloud have been used. In this case the cloud characteristics are selected by the test condition and are defined by the values of LWC and MVD. The first parameter affects strongly the quality of the measurements because for the highest values of the cloud concentration the measurement area is blinded. Another aspect to be taken into account is the quality of the optical access to the tunnel, due to high cloud concentration values or strong wake condensation appears on the windows. Heating or purge systems are adopted in order to avoid moisture on the optical windows.

### 3. Experimental test

Hereinafter two different experimental campaign are described.

#### 3.1 PIV assessment in CIRA IWT

The first campaign has been performed on April 2005. It was aimed to demonstrate the applicability of PIV in CIRA-IWT and to individuate the limits of the operating conditions in terms of cloud characteristics, static temperature, static pressure and wind speed. For this first entry the secondary TS ( $2.35 \times 1.15 \times 5 \text{ m}^3$ ) has been selected due to the fact that it presents the extreme condition in term of wind speed, and static temperature. The measurement zone has been set in concomitance of the centre longitudinal plane. The reference system has been set with the origin on the bottom centre line of the TS, the x axes directed versus the wind velocity, the z axes toward the wall ceiling. The laser head was mounted on the test chamber ceiling, and the light sheet was vertically directed trough an available window. An area of  $420 \times 340 \text{ mm}^2$  has been acquired with a single camera with a 60mm lens located outside the side wall. Tests have been conducted at 100, 120 and 148 m/s wind speed in free stream condition. In order to validate protection system, tests have been performed at various static temperature ( $-4^\circ$ ,  $-25^\circ$  and  $-30^\circ \text{ C}$ ) and at two total pressures (110.000 and 53846 Pa). Particular care has been taken in investigating PIV system behaviour for different cloud condition. The droplets diameter (MVD) has been varied in the range from 15 to 250  $\mu\text{m}$  while the concentration (LWC) has been set in the range from 0.15 to 2.8  $\text{g}/\text{cm}^3$ . Measurements in the wake of the icing blade probe has been performed as well in order to evaluate possible problems arising from wake condition. For each test condition 150 instantaneous velocity fields have been acquired. Ensemble average velocity field and relative turbulence level field has been evaluated by the total sample available for each test condition.

#### 3.2 Performance degradation investigation

The second test campaign has been performed on January 2006. It was aimed to investigate the real potentiality of PIV in the framework of an icing test. The test foresaw the installation on the IWT of the largest test section (additional  $2.35 \times 3.6 \times 8.3 \text{ m}^3$ ) together with a full scale wing tip with movable slat. Two different model configurations have been simulated: high lift and cruise condition. For both the configurations, tests with and without ice accretion have been conducted at respectively static temperature of  $-1^\circ \text{C}$  and  $-5^\circ \text{C}$ . A fixed LWC value of  $1 \text{ g}/\text{m}^3$  and two MVD values (10 and 27  $\mu\text{m}$ ) have been selected in order to investigate the influence on the behaviour of the water droplet trajectories. PIV measurement has been carried out during ice accretion for 15 minutes with a 0.5 Hz of frame rate.

The high lift model configuration foresaw an angle of attach of  $3.5^\circ$  and a  $32^\circ$  of slat deflection angle. Two cameras have been aimed to the slat wing gap region. The measurement plane has been located orthogonal to the wing leading edge. One camera was equipped with a 60mm focal lens covering all the region up stream the slat whereas the second camera mounting a 100mm lens has been focused on the intersection region. The recording areas were respectively  $340 \times 270 \text{ mm}^2$  and  $200 \times 160 \text{ mm}^2$ . The reference system has been positioned with the origin in the intersection between the light sheet and the slat trailing edge, x axes directed orthogonal to the TE toward the main speed

direction, z axes was positioned vertical toward the ceiling wall and y axes parallel to the TE. The two fields of view presented an overlap region. Figure 9 shows the location of the recording areas. The laser as in the previous case was located above the test chamber (figures 5-6) .



**Figure 9: PIV recording set up on the LE**

The cruise configuration foresaw  $0^\circ$  degree of incidence angle and slat retracted. Also in this case two cameras have been used. The cameras have been located at about two chords downstream the trailing edge of the wing. In order to cover the entire wake region the cameras have been mounted vertically with an overlap in the recording region. The cameras mounted 60 mm focal length lenses providing a recording area of  $276 \times 220 \text{ mm}^2$  each. The region of interest has been located in the longitudinal centre line plane. Figure 10 shows the experimental set up adopted for the characterisation of the wake.



**Figure 10: Recording camera and experimental set up in the wake region**

## 4. Results and discussions

In the following the main results are presented and discussed. As it is possible to deduce from the test description from the previous section, a considerable amount of data was acquired. So far, in the following only an overview is reported.

### 4.1 PIV Assessment

PIV measurements have been performed for several cloud configurations in free stream condition. All the condition of speed, static temperature and static pressure have been fulfilled. The only encountered limitation was on the composition of the cloud. A LWC value of  $2.0 \text{ g/m}^3$  has been found being the upper level limit for good quality PIV images. The tests performed at higher values of LWC, have generated clouds with concentration that not allowed to detect the particles in the measurements area. In Figure 11 the ensemble average U component of the velocity field and the relative turbulence level versus the z axes are reported. The test has been carried out at  $100 \text{ m/s}$  wind tunnel speed,  $15 \text{ }\mu\text{m}$  of MVD and  $0.15 \text{ g/cm}^3$  of LWC. Comparison at different location along

the x direction is reported. U velocity component shows a good uniformity long z direction and for different station long x axes. The Relative Turbulence Level (RTL) behaviour obtained with PIV is compared with a measurement point obtained performing hot wire anemometry measurements in the air. The slight underestimation is explained by the velocity lag induced by the mass of the particle characterised by a mean diameter of 15  $\mu\text{m}$ . This foresees a reduction of the velocity fluctuation.

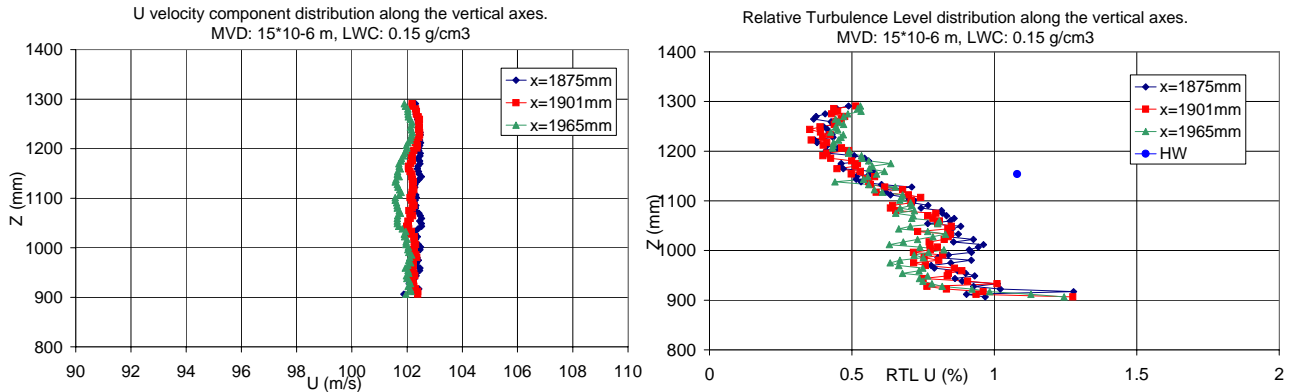


**Figure 11: U velocity comp. and RTL distribution along the vertical axes in free stream condition.**

The second configuration foresaw to apply PIV technique to a typical condition arising during aerodynamic test, i.e. the wake characterisation. In case of icing test, low temperature and high humidity the wake is affected by condensation phenomena as is visible in Figure 12. The image clearly show a white zone induce by the wake, this brighter background can affect the quality of the signal to noise ratio.



**Figure 12: Flow field picture of the wake behind the icing blade**

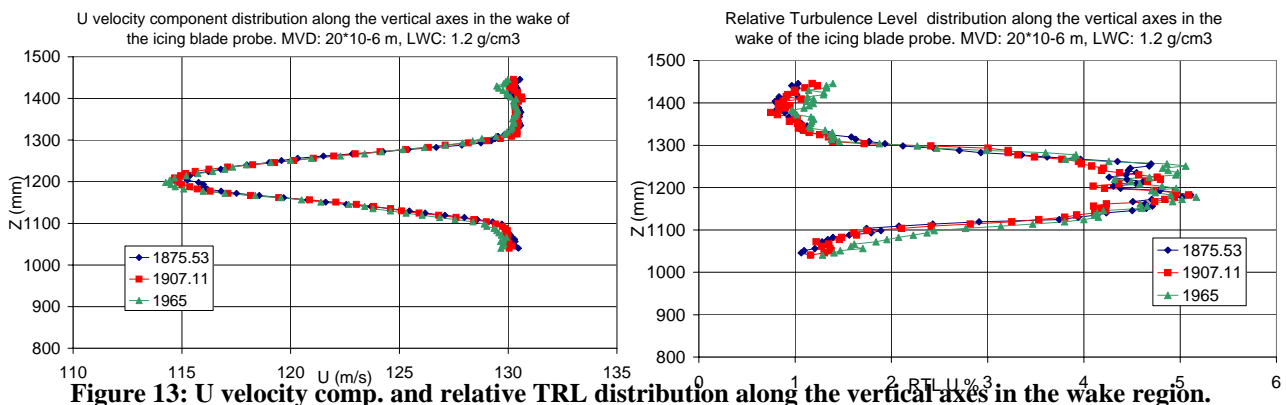


**Figure 13: U velocity comp. and relative TRL distribution along the vertical axes in the wake region.**

Figure 13 presents the U component of the ensemble average velocity field and the RTL versus the z direction measured in the wake of the icing blade. The result correspond to a test condition of 125 m/s, -30°C static temperature, cloud characteristic of 20 μm of MVD and 2.0 g/cm<sup>3</sup> of LWC. The diagrams show the typical lost of momentum induced by the wake. The RTL starting from the undisturbed value of 1% increases in the wake up to a value of 5%.

#### 4.2 Performance degradation investigation

The first measurements have been carried out at -1° C temperature value in order to avoid ice formation on the model and 60 m/s of wind velocity. The droplets trajectories on the leading edge zone of a complex model in high lift configuration has been measured for two different values of droplets diameter (15 and 27 μm MVD). In figure 14 the model zone interested by the PIV measurement are visible. On the geometry of the model with 3.5 ° degree of AoA and -32° degree of slat deflection the ensemble average velocity field obtained on 150 instantaneous samples has been over imposed. A detail of the PIV results is shown in figure 15. The figure presents the droplet trajectory evaluated on the mean velocity field. Starting from the trajectories it is possible to evaluate the global collection efficiency (E) defined as the ration between the mass water droplets impinging and the mass water seen in the body projected area. This value is obtained integrating on the leading surface of the model the local collection efficiency (β) defined as the ratio between the

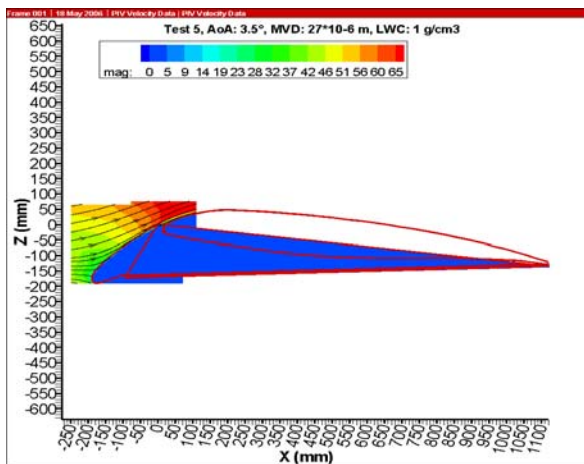


Figure 14: PIV measurement areas

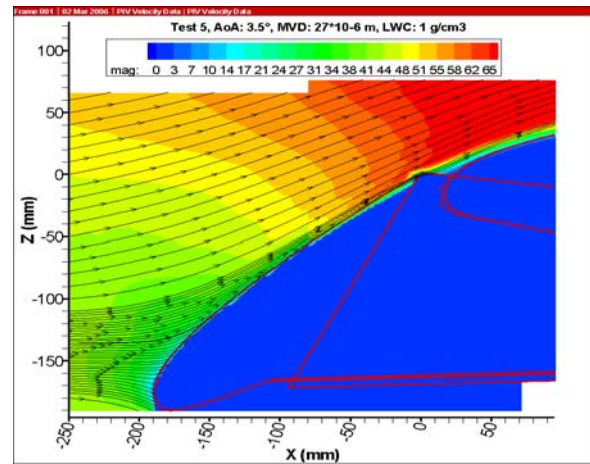


Figure 15: Droplet trajectories and velocity field colour map

space (dz) between two side stream line upstream the body in the undisturbed zone and the distance on the body surface where the trajectories impact (ds), i.e.  $\beta = dz/ds$ . The local value of the collection efficiency has been evaluated for 15 and 27 μm MVD. The results are shown in Figure 16.

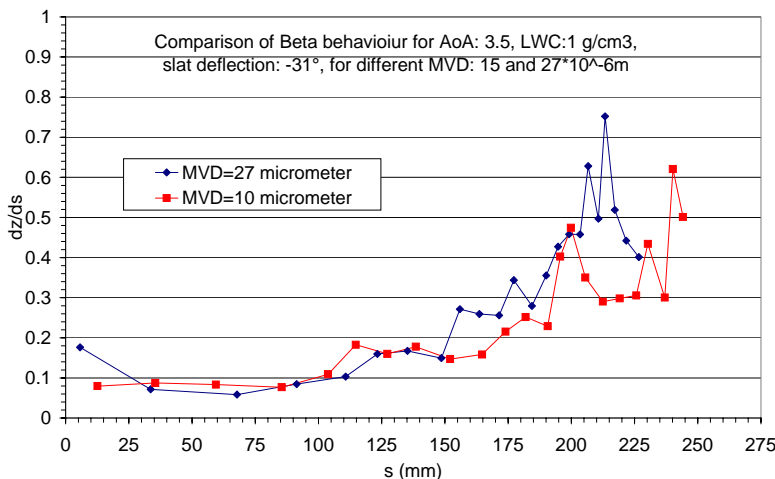


Figure 16: Collection efficiency versus surface coordinate.

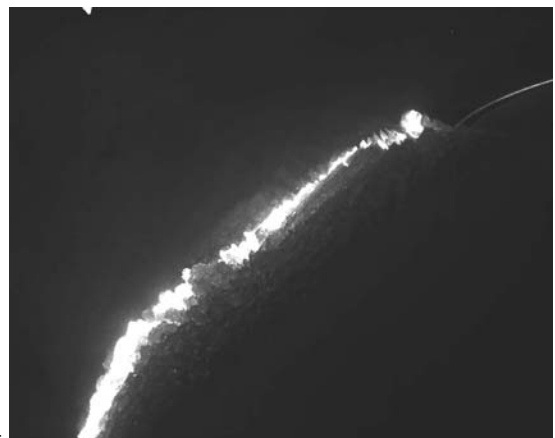


Figure 17; PIV image during ice accretion

Beta has been evaluated on the slat surface, imposing the origin in the slat T.E. and moving toward the L.E. The diagram presents as expected an increasing of the value of beta moving toward the leading edge. The curve relatives to the larger droplets diameter shows an higher value of beta. This is due to the inertia force of the droplet, the trajectories are less influenced by the presence of the model and consequently a larger ice accretion occurs.

In order to allows the ice formation on the model the static temperature has been dropped down to -5°C. The condition selected: 27  $\mu\text{m}$  of MVD and 1.0  $\text{g}/\text{cm}^3$  of LWC correspond to a glaze ice shape.

This type of ice accretion is the worst that can occurs in term of aerodynamic performance degradation altering the profile shape and in term of PIV recording because the ice is bright and highly reflective as shown in figure 17. The detection of the ice shape profile is quite challenging due to the non uniformity of the ice formation long the span wise, so it occurs that ice formation covers the measurement area and strong reflection inside the ice affect the quality of the PIV images close to the ice formation. Figure 18 shows the formation of ice after 15 minutes of flight trough the cloud.



Figure 18: Front and side view of the wing after the accretion of the ice

PIV data have been recorded with a frequency of 0.5 Hz. In Figure 19 the results obtained by the analysis two PIV images recorded respectively after 5 and 15 minutes from the beginning of the ice accretion on the wing. It is clearly visible the disturb on the stream lines due to the ice presence (for comparison see the results shown in figure 15). The zone blue coloured in front the slat profile represent the ice accretion shape obtained by tracing the PIV image. From the two colour maps it is also visible the increasing of the ice thickness with the passing time.

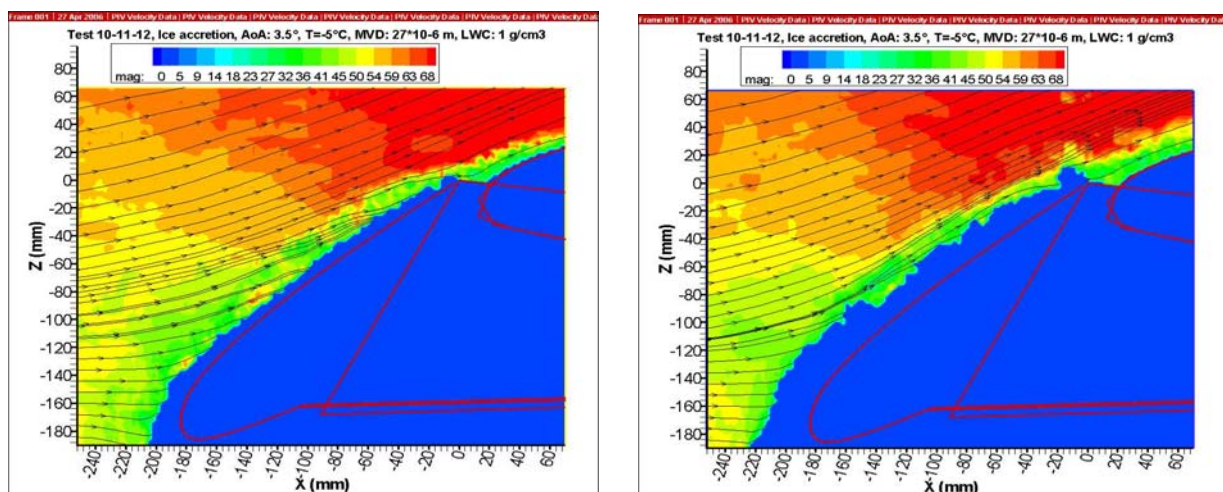
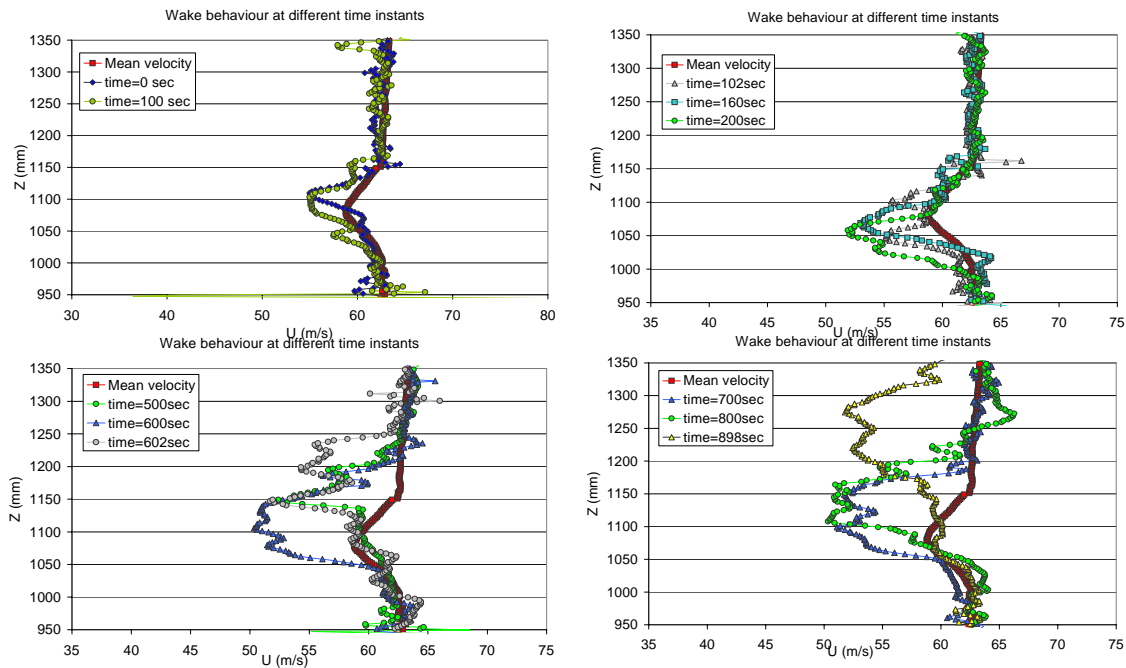


Figure 19: PIV results obtained respectively after 5 and 15 minutes from the start of the ice accretion.

The tracing of the ice shape is still affected by large error due to the strong laser light scattering, but

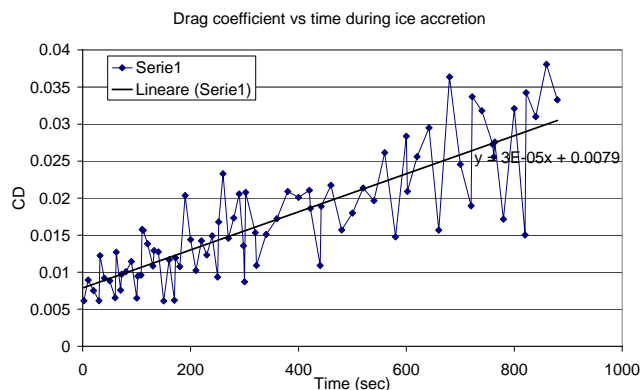
it is a big step forward because actually information on the ice shape is possible to have only at the end of the run and by a manually tracing. Activities are in progress for increasing the quality of the recorded image. The wake measurements have been performed with the model in cruise configuration. The test conditions were the same of the high lift configuration. Measurements during the ice accretion phase have been carried out for 15 minutes with 0.5 Hz recording frequency.

Figure 20 shows the wake behaviour at different instant during the ice accretion. In each diagrams the value of the wake obtained for the case of clean profile averaging on 150 samples is compared with the single wake obtained by the instantaneous velocity fields at different instant. It is clearly detectable the increasing of the ice effect up to the flow separation occurs. The typical separated flow behaviour occurs starting from 500 sec. after the beginning of ice formation, it is indicated by the double peak typical of the vortex shedding induced by the flow separation.



**Figure 20: Wake behavior at different time instant during ice accretion**

Starting from the wake flow field characterisation a first attempt to measure the drag coefficient has been carried out using a simplified method for 2D profiles, due to the fact that the third component of velocity was not available. Figure 21 presents the drag coefficient behaviour at different instant since the starting of the ice accretion. The scattering of the data is due to the fact that the CD as been obtained on single instantaneous velocity field, highly unsteady. The diagram presents an uniform trend, as the time passes, and consequently the ice accretes, the drag coefficient increases almost linearly.



**Figure 21: CD behavior versus time accretion**

## 5. Conclusions

The assessment of PIV technique in an icing wind tunnel has been demonstrated for the first time. The measurements were effective in the following range of application: Wind speed up to 150 m/s, MVD range: 15 to 250  $\mu\text{m}$ , LWC range: 0.15 to 2.0  $\text{g}/\text{cm}^3$ , Altitude: 0 to 6000 m on s.l., Static temperature: 0° to -30°C.

Several measurement campaigns have been performed in order to investigate the range of applicability of PIV and the potentiality of the technique.

PIV technique allowed to evaluate, using the water cloud as seeding, the droplet trajectories and the collection efficiency on the model. Using standard PIV is possible to evaluate the flow stream lines and in this way is possible to measure the different behaviour with the water droplet trajectories. These measurements provide unique data for CFD validation.

The wake measurement allows to measure, by means the lost of momentum, the increasing of drag coefficient due to the ice accretion.

Some problems are still present, the strong light scattering due to the ice formation on the model affect the quality of the result in proximity of the model. The background noise due to the water droplets run back on the model provides spurious vector in the final results. Methods to eliminate or to reduce the laser light scattering are under studying. In case of succeeding together with the improvement of the quality of the PIV results shall be possible to measure quantitatively also the ice accretion on the model continuously, operation at nowadays it is only possible at the end of the test run performing a manual tracing of the ice formation

## Acknowledgements

This work has been partially founded in the framework of the project ACADEMIA sponsored by the Italian University and Scientific Research Ministry. The author wish to acknowledge the valuable contribution enabling the success of this investigation by: the IWT crew and in particularly by M. Bellucci, G. Esposito and M. Lupo.

## References

- Preston, G.M. and Blackmann, C.C. (1948) Effects of Ice Formation on Airplane Performance in Level Cruise Condition. NACA TN 1598
- Leckman, P.R. (1971) Qualification of a Light Aircraft for Flight in Icing Condition. SAE paper N. 710394
- Bragg M.B., Hutchison T., Merret J., Oltman R., Pokhariyal D. (200) Effect on Ice Accretion on Aircraft Flight Dynamics. AIAA 2000-0360
- Bragg, M.B., Gregorek, G.M., (1992) Aerodynamic Characteristics of Airfoils with Ice Accretions. AIAA 20<sup>th</sup> Aerospace Sciences Meeting, January 11-14, Orlando, Florida
- Bragg, M.B., Coirier, W.J., (1986) Aerodynamic Measurements on an Airfoil with Simulated Glaze Ice, AIAA 24<sup>th</sup> Aerospace Sciences Meeting, January 6-9, Reno, Nevada
- Cuerno, C., Martinez-Val, R., Perez, A. (1997) Experimental Diagnosis of the Flow around a NACA 0012 Airfoil with Simulated Ice. Proc. 7<sup>th</sup> Conference of Laser Anemometry Advanced and Application, Karlsruhe, Germany, pp. 747-754.
- De Gregorio F., Ragni A., Aioldi M., Romano G.P. (2001) PIV Investigation on Airfoil with Ice Accretion and Resulting Performance Degradation. Proc. 19<sup>th</sup> ICIASF, Cleveland, Ohio, pp 94-105.